Field Implementation of a Winsor Type I Surfactant/Alcohol Mixture for in Situ Solubilization of a Complex LNAPL as a Single-Phase Microemulsion

JAMES W. JAWITZ,[†]
MICHAEL D. ANNABLE,*,[†]
P. S. C. RAO,[†,‡] AND R. DEAN RHUE[‡]

Interdisciplinary Program in Hydrologic Sciences, University of Florida, Gainesville, Florida 32611

A Winsor Type I surfactant/alcohol mixture was used as an in situ flushing agent to solubilize a multicomponent nonaqueous phase liquid (NAPL) as a single-phase micro-emulsion (SPME) in a hydraulically isolated test cell at Hill Air Force Base (AFB), Utah. The surfactant (polyoxy-ethylene(10) oleyl ether) and alcohol (1-pentanol) together comprised 5.5 wt % of the flushing solution. The NAPL was extremely complex, containing more than 200 constituents and a 'pitch' fraction that was not solvent-extractable. The NAPL removal effectiveness of the SPME flood was evaluated using information from soil cores, partitioning tracer tests, and NAPL constituent breakthrough curves (BTCs) measured at three extraction wells. Soil core data indicated that approximately 90−95% of the most prevalent NAPL constituents were removed from the cell by the SPME flood. A comparison of pre- and postflushing partitioning tracer data indicated that about 72% of the measured NAPL volume was removed by the SPME flood. Integration of NAPL constituent BTCs indicated 55−75% removal of the target NAPL constituents when partitioning tracer data were used to estimate the initial amount of NAPL present and 60−175% removal of two target constituents when soil core data were used to estimate the amount of NAPL initially present. These results indicate that the SPME flood effectively removed the NAPL constituents of concern, but an insoluble anthropogenic residue was left behind.

Introduction

Recently, many investigators have demonstrated that in situ flushing techniques show promise for the remediation of aquifers contaminated with nonaqueous phase liquids (NA-PLs), such as fuels and chlorinated solvents, in time frames much smaller than would be expected for traditional pump-and-treat methods (*1−4*). Similar to enhanced oil recovery (EOR) (*5, 6*), these flushing technologies generally involve the addition of chemical agents to an injection fluid during either miscible or immiscible displacements to accelerate the dissolution or displacement of NAPLs from contaminated

aquifers. Two classes of chemical agents used for in situ flushing that have been the focus of much study are cosolvents (*7−10*) and surfactants (*3, 11−14*).

Both cosolvent and surfactant solutions can be used to accelerate the removal of residually trapped NAPLs from porous media through either mobilization or enhanced solubilization. Mobilization of NAPL trapped within the porous media by capillary forces is facilitated by a reduction in the interfacial tension (IFT) between the NAPL and the flushing solution as either a cosolvent or surfactant solution displaces the resident groundwater and contacts NAPL ganglia. Similarly, solubilization of the NAPL is enhanced due to the reduced polarity of the flushing solution as compared to that of the resident groundwater.

Several laboratory and field mobilization studies have shown that a large percentage of the NAPL trapped in contaminated porous media, often >95%, can be removed after injecting a small number of pore volumes (PV) of flushing fluid (*2, 15, 16*). However, mobilization technologies are limited to sites where the flow of the mobilized NAPL can be controlled and the potential for migration of NAPL through layers that previously acted as capillary barriers can be assured. Remediation technologies that rely on solubilization generally do not remove the NAPL as efficiently as mobiliza-tion technologies. However, solubilization technologies generally pose less risk with regard to uncontrolled migration of the mobilized NAPLs and are less complex to design, particularly with regard to the number of parameters requiring optimization. It is for these reasons that our focus has been on developing aquifer remediation strategies that solubilize NAPLs without inducing mobilization (*9, 17−19*).

The results reported here are from a field-scale aquifer remediation study conducted in a surficial aquifer contami-nated with a complex NAPL mixture, wherein NAPL solu-bilization without mobilization was the goal. This study was one of eight pilot-scale tests funded by the Strategic Environmental Research and Development Program (SERDP) and the Advanced Applied Technology Demonstration Facil-ity (AATDF) and conducted side-by-side at Hill Air Force Base (AFB), UT, for the purpose of evaluating in situ flushing remediation technologies for the removal of NAPLs from subsurface environments. In this study, we used a surfactant/ alcohol mixture to generate a Winsor Type I system, where the NAPL was solubilized and transported as a single-phase microemulsion (SPME). For the SPME process, only 5.5 wt % of the flushing solution was comprised of chemical additives.

The SPME flushing study was conducted in a hydraulically isolated test cell (2.8 m × 4.6 m), similar in design to that described by Rao et al. (*1*). The amount and spatial distribution of residual NAPL within the test cell were determined both before and after SPME flushing using soil cores and interwell partitioning tracer tests (*20, 21*). During the SPME flood, fluid samples were regularly collected from extraction wells and were analyzed for target NAPL con-stituents. This paper will focus on interpretation of data from soil cores, partitioning tracer tests, and extraction well samples for the evaluation of the NAPL removal effectiveness of the SPME flushing experiment.

Technology Description. A microemulsion is an optically transparent dispersion of liquid droplets (<0.1 μm) sus-pended within a second, immiscible liquid stabilized by an interfacial film of surface-active molecules (*22*). Generally, the stabilizing interfacial film is comprised of both a surfactant and a cosurfactant (such as an intermediate chain-length alcohol). Varying a parameter that changes the character of

* Corresponding author Phone: (352) 392-3294; fax: (352) 392-3076; e-mail: manna@eng.ufl.edu.
† Department of Environmental Engineering Sciences.
‡ Soil and Water Science Department.

TABLE 1. Mass Fractions of Target NAPL Constituents and Mass of Each Constituent Removed from the Extraction Wells during SPME Flushing

NAPL constituent	mass fraction, X_i [a] (g/100 g of NAPL)	log K_{ow} [b]	mass removed during flushing			
			EW 1 (kg)	EW 2 (kg)	EW 3 (kg)	total (kg)
p-xylene	0.144	3.15	0.104	0.097	0.100	0.301
1,2,4-trimethylbenzene	0.438	3.63	0.370	0.366	0.387	1.123
n-decane	0.477	6.25	0.408	0.367	0.346	1.121
n-undecane	1.573	6.53	1.130	1.005	0.982	3.117
n-dodecane	0.698	6.80	0.492	0.442	0.414	1.348
n-tridecane	0.285	7.40	0.257	0.238	0.203	0.697

[a] Measured by dissolving NAPL collected from the field site in hexane and analyzing by GC with flame ionization detection (19). [b] From Sangster (33), except n-undecane and n-tridecane values, which were estimated based on interpolation.

the system from hydrophilic to lipophilic will produce a phase transition from an oil-in-water microemulsion (oil, or NAPL, droplets in a water-continuous phase; Winsor Type I) to a water-in-oil microemulsion (water droplets in an oil phase; Winsor Type II). Winsor Type III systems are formed midway in the transition from hydrophilic to lipophilic systems. At the transition to a Winsor Type III system, the IFTs between the microemulsion phase, also known as the middle phase, and any excess oil or water phases present reach extreme minimums, much lower than those achieved in Winsor Type I and II systems. It is because of these ultralow IFTs that middle-phase microemulsions have been promoted for both EOR (5, 6) and aquifer remediation via NAPL mobilization (2, 14, 16, 23). However, middle-phase systems can be difficult to design in field settings because of the relatively large number of parameters requiring optimization (e.g., salinity, surfactant concentration, and aquifer geochemical conditions) (16, 24).

Martel and collaborators (25, 26) proposed the use of Winsor Type I microemulsions to solubilize NAPLs without mobilization. These systems have the advantage of high solubilization of NAPLs (although not as high as middle-phase microemulsions) with relatively low amounts of chemical additives required. Chun-Huh (27) showed that, in microemulsions, solubilization of the oil phase into the microemulsion is related to interfacial tension by an inverse-squared relationship. Therefore, remediation systems that rely on Winsor Type I microemulsification will necessarily be less efficient than those that rely on Winsor Type III microemulsions and mobilization, since solubilization will be lower at the higher interfacial tensions required to prevent mobilization.

The first phase of this study was to select a surfactant and cosurfactant, which together form the microemulsion precursor, that would produce a low-viscosity, single-phase microemulsion on contact with the multicomponent NAPL found at the field site. Eighty-six surfactants and a number of alcohols were screened, with maximum NAPL solubilization and low viscosity (<2 cp) as the main acceptance criteria (19). The viscosity of the precursor solution was limited to preclude large hydraulic gradients across the test cell and excessive drawdown around the extraction wells. The precursor solution selected was the surfactant Brij 97 (polyoxyethylene(10) oleyl ether) at 3% by weight and 1-pentanol at 2.5% by weight in water. Rhue et al. (19) found that, upon equilibration of the SPME precursor solution with the NAPL from the field site, the dissolved concentration of dodecane was 104 mg/L as compared to an expected aqueous concentration of 2.6×10^{-5} mg/L (based on an aqueous solubility of 0.0037 mg/L and a mass fraction in the NAPL of 0.698 wt %, Table 1). Greater NAPL solubilization could be achieved with higher concentrations of surfactant and cosurfactant. However, increased solubilization would be accompanied by a concomitant increase in viscosity. The field-measured viscosity of the precursor was 1.66 cp.

Field Site Description. A brief summary of the field site history and geohydrology follows; greater detail can be found in a report written for Hill AFB by Montgomery Watson, Inc. (28). Hill AFB is located approximately 50 km north of Salt Lake City, UT. The field site is located in a NAPL source zone within a shallow surficial aquifer. The aquifer material consists of sand and gravel (Provo Formation), with a thick (>60 m) clay aquitard (Alpine Formation) approximately 8 m below ground surface (bgs). The aquifer was contaminated through the use of two chemical disposal pits in the 1940s and 1950s. A variety of liquid wastes such as fuels, waste oils, and spent solvents from degreasing operations were disposed of in these pits. Migration over the years has caused the spreading of the NAPL source zone to an area of approximately 2.8 ha.

The NAPL collected from wells at the site is a very hydrophobic mixture that tends to strongly coat solid surfaces. Although only a handful of constituent compounds are discussed here, more than 200 have been identified (28). However, NAPL collected at the site was completely miscible with both hexane and methylene chloride. The NAPL density was measured to be 0.88 g/mL, and it is thus generally found at or above the water table (approximately 7 m bgs). Periodic water table fluctuations since the contamination events have created a NAPL smear zone extending up approximately 3 m from the clay layer (i.e., 5−8 m bgs). For the experiments reported here, the water table within the cell was maintained at 4.9 m bgs in order to capture the entire NAPL smear zone within the flow domain (see Supporting Information and Figure 4).

Methods

A summary of the experimental methods follows. Additional details about the test cell design, fluid delivery and mixing systems, tracer test and soil sampling procedures, and analytical methods can be found in the Supporting Information.

Test Cell Design and Instrumentation. The design of the eight hydraulically isolated test cells at the SERDP site was similar to that of the cell which was built for the University of Florida (UF)/EPA cosolvent flushing project conducted within the same NAPL source plume at Hill AFB in 1994−1995 (1, 21). The cells were constructed of interlocking steel sheet piles with grouted joints, enclosing rectangular areas of approximately 2.8 m × 4.6 m and penetrating from the ground surface to approximately 3.7 m into the clay confining unit. The Z-shape of the individual piles resulted in corrugations around the perimeter of the cell (Figure 1) that represented approximately 17% of the cell area. The instrumentation of each cell was similar to that described by Annable et al. (21), with four injection wells (IWs) and three extraction wells (EWs), all fully screened, and a network of spatially distributed multilevel samplers (MLSs) that resulted in 96 individual sampling points (Figure 1). A leak test
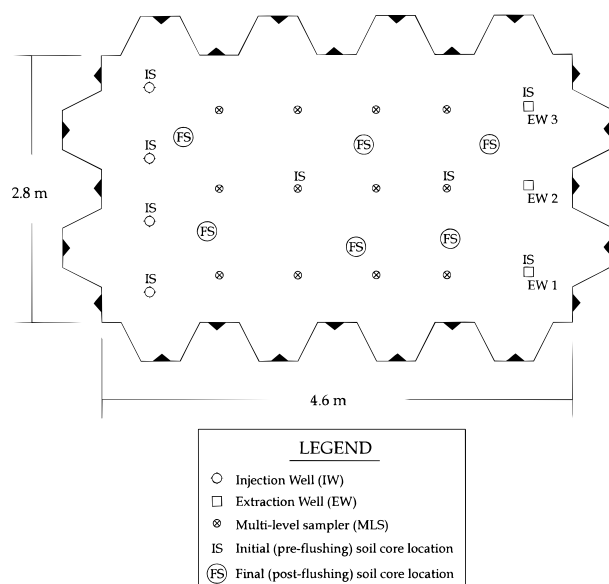
FIGURE 1. Plan view of cell layout. Solid triangles represent grout-filled joints between individual interlocking sheet piles. All preflushing soil cores were taken during installation of wells and MLSs at the indicated locations.

conducted within the cell showed losses of less than 0.3% of the pore volume per day.

Hydrodynamics Characterization. A nonreactive tracer test was conducted to characterize the test cell hydrodynamics prior to partitioning tracer tests and SPME flushing. The effective pore volume of the test cell was determined to be approximately 6.0 kL based on moment analysis (*29*) of nonreactive tracer breakthrough curves (BTCs) measured at the extraction wells. The effective porosity within the test cell was measured to be 0.14 by both hydraulic testing and the nonreactive tracer test. Also, the average hydraulic conductivity across the cell was determined to be 0.01 cm/s by measuring the hydraulic gradient between two piezometers, set 1.6 m apart along the flow direction, at different flow rates.

NAPL Saturation and Spatial Distribution Characterization. The preflushing distribution of target NAPL constituents was determined from 85 soil samples collected from eight borings, and the postflushing distribution was determined from 40 subsamples collected from six borings (Figure 1). For consistency in the evaluation of the remediation effectiveness of the eight SERDP/AATDF pilot tests, soil samples collected from each test cell were analyzed for the same 12 NAPL constituents (*28*). Of these 12 constituents, the seven found to be most prevalent in our cell are listed in Table 2, while the following five were found to have average soil concentrations of less than 0.1 mg/kg: 1,1,1-trichloroethane, trichloroethene, benzene, toluene, and ethylbenzene.

The amount and spatial distribution of residual NAPL present before and after SPME flushing were estimated using interwell partitioning tracer tests conducted with methods similar to those described by Annable et al. (*21*). For both the pre- and postflushing tracer tests, a tracer pulse of 0.16 PV was delivered to the injection wells during steady water flow of approximately 1 PV/day (3.6 L/min), with methanol (C_o = 2700 mg/L) and 2,2-dimethyl-3-pentanol (2,2-DMP; C_o = 930 mg/L) as the nonpartitioning and partitioning tracers, respectively. To accurately characterize the BTC tails, where much of the measured retardation is often found, both the pre- and postflushing tracer tests were continued until tracer concentrations at the EWs were below the detection limits (approximately 1 mg/L) and tracer BTC tails were exponentially extrapolated (*13*). Moment analysis was

performed on BTCs generated at the EWs to determine well swept volumes and NAPL saturations using relationships presented elsewhere (*20, 21*). The NAPL−water partitioning coefficient, K_N = 10.7, for 2,2-DMP was measured using batch equilibration methods.

Microemulsion Flushing. The microemulsion flushing field experiment consisted of pumping 9 PV (54.3 kL) of precursor solution through the test cell over a period of 18 days, followed by 1 PV of a surfactant-only flood, and 6.5 PV of water flooding. The designed duration of the experiment was based upon laboratory column studies conducted by Rhue et al. (*19*) with contaminated soil from Hill AFB, wherein after approximately 5 PV of SPME flushing, NAPL constituents were no longer being eluted from the soil. We increased this approximately 2-fold to account for greater hydrodynamic dispersion expected as a consequence of field-scale heterogeneities.

Because the 12 analytes selected as indicators for comparison of the 8 SERDP/AATDF pilot tests were not the most prevalent constituents in the NAPL found in our cell, Rhue et al. (*19*) selected nine constituents that (a) produced large peaks in a GC−FID chromatogram of NAPL from our cell that had been dissolved in hexane and (b) were representative of different contaminant types. These nine constituents included the six compounds listed in Table 1 and 1,2,4-trichlorobenzene (TCB), 1,2-dichlorobenzene (DCB), and naphthalene. Fluid samples collected at the EWs and MLSs during the flushing experiment were shipped overnight to UF and were analyzed by GC−FID for these nine target NAPL constituents. The extraction well data for TCB, DCB, and naphthalene are not presented here because chromatographic peak overlapping led to unreliable results.

Waste Management and Minimization. The extraction fluid waste was characterized as either low level or high level. Fluids extracted from the test cell that were representative of groundwater contamination at the site and fluids containing low levels of injected tracers were characterized as low-level waste. Effluent that was extracted from the cell during the SPME flushing process was characterized as high-level waste. Both categories of waste were approved for discharge to the industrial wastewater treatment plant at Hill AFB. However, because of its high chemical oxygen demand, the high-level waste discharge was metered over a period of 30 days.

Performance Effectiveness Measures. Rao et al. (*1*) used extraction well mass balances and pre- and postflushing data from groundwater samples, soil cores, and partitioning tracer tests to characterize the NAPL removal effectiveness of the UF/EPA in situ cosolvent flushing experiment. The NAPL removal effectiveness of the SPME flood was determined from the fraction reduction in NAPL saturation, as measured by partitioning tracer tests, and by the fraction reduction in the cell-average soil concentrations of several NAPL constituents, as determined from soil core analyses. In addition, NAPL constituent BTCs were integrated to determine the total mass of each contaminant removed during SPME flushing. These values were compared to estimates of the initial amount of NAPL present as determined from both partitioning tracer tests and soil cores.

Groundwater samples were collected from 84 MLSs both before and after SPME flushing and were analyzed for all 12 analytes monitored in the soil samples, except for the very slightly soluble *n*-decane and *n*-undecane, using headspace gas chromatographic techniques (see Supporting Information). However, all but seven of the groundwater samples resulted in nondetects, most likely because these constituents were present in our cell in only very small quantities (see Table 2). Therefore, data from the groundwater samples were not used to evaluate the effectiveness of the SPME flood.

TABLE 2. Pre- and Postflushing Average Soil Concentrations of Target NAPL Constituents

NAPL constituent	average soil concentration (mg/kg)[a]		fraction reduction[d]
	preflushing[b]	postflushing[c]	
n-undecane	61.2 ± 51.6	2.51 ± 5.87	0.96 ± 0.10
n-decane	24.9 ± 21.2	1.10 ± 2.71	0.96 ± 0.12
1,3,5-trimethylbenzene	2.90 ± 2.49	0.25 ± 0.89	0.92 ± 0.31
naphthalane	0.91 ± 1.23	0.11 ± 0.27	0.88 ± 0.34
1,2-dichlorobenzene	0.74 ± 1.99	0.03 ± 0.08	0.96 ± 0.16
o-xylene	0.18 ± 0.31	0.06 ± 0.09	0.65 ± 0.79
m-xylene	0.12 ± 0.15	0.02 ± 0.04	0.87 ± 0.39

[a] Values are arithmetic averages with standard deviation, where standard deviation represents the spatial variability. [b] Of the 83 samples, $n = 59$ were from within the swept zone. [c] $n = 36$. [d] Fraction reduction determined from $(C_i - C_f)/C_i$, where C_i is the preflushing average concentration and C_f is the postflushing average concentration. Standard deviation of fraction reduction determined by propagating pre- and postflushing standard deviations, STD_i and STD_f, respectively, using $[(C_f STD_i/C_i^2)^2 + (STD_f/C_i)^2]^{1/2}$.
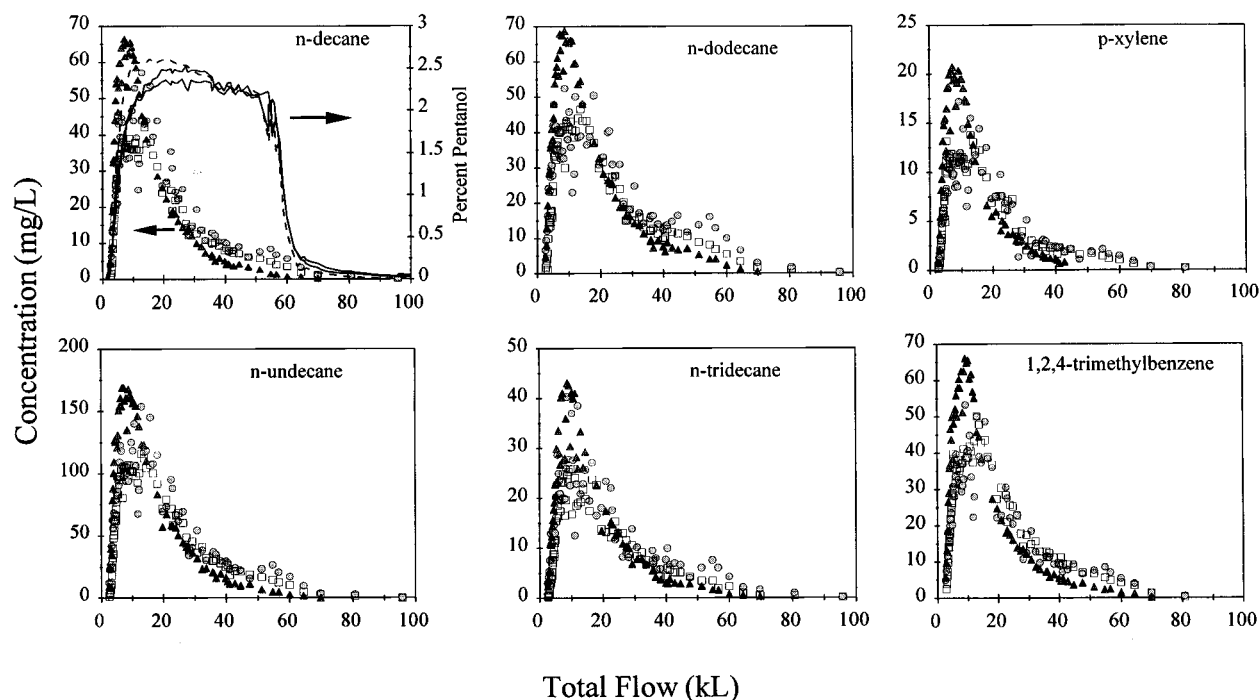
FIGURE 2. BTCs for target NAPL constituents measured at EW 1 (○), EW 2 (▲), and EW 3 (□). Overlain on the *n*-decane graph are the 1-pentanol breakthrough data (solid lines for EWs 1 and 3, dashed line for EW 2).

Results

Extraction Well BTCs. *SPME Hydrodynamic Considerations.* Analytical interferences with NAPL constituents precluded analysis of effluent samples for surfactant concentrations. Therefore, precursor arrival at the extraction wells was inferred from 1-pentanol arrival. This assumption was based on laboratory column studies (*19*) using soil from the field site, which indicated no chromatographic separation of surfactant and pentanol. Also, the 1-pentanol arrival time at the EWs during the SPME flood was equivalent to the arrival time of the nonpartitioning tracer (methanol) during the postflushing tracer test, indicating no significant retardation of the 1-pentanol. The 1-pentanol BTCs measured at the three EWs are overlain on the first target analyte BTC (*n*-decane) in Figure 2 (1-pentanol injection and elution profiles are presented in full in the Supporting Information). The BTCs in Figure 2 are plotted in terms of the total flow through the entire test cell (total flow); all other BTCs presented here are plotted as the flow through an individual well (local flow). The 1-pentanol BTCs from EWs 1 and 3 were very similar, while that of EW 2 was steeper, indicating less tailing on the frontal rise. The corrugations of the sheet-pile walls contributed to longer flow paths in the swept

volumes of the two outer wells (EW 1 and EW 3) than in the swept volume of the centerline well (EW 2), leading to greater tailing in the BTCs at the outer wells. This behavior is also exhibited in the nonpartitioning tracer BTCs discussed below.

NAPL Microemulsification. Breakthrough curves for target analytes measured at the EWs (Figure 2) represent NAPL constituent removal over the entire swept volume of the fully screened wells (*1*). For each target constituent, a significant increase was observed in the effluent fluid concentrations as compared to the pre-SPME flood concentrations. The increase in *n*-decane concentration is shown to be coincident with the arrival of the precursor solution; a similar trend was observed for all analytes. The NAPL constituent BTCs were integrated to determine the total mass of each contaminant removed from the swept volume of each of the EWs (Table 1). The amount of mass removed from each well was similar, with a trend of greater mass removed from EW 1 than from EWs 2 and 3.

For all analytes, the BTCs measured at EW 2 showed higher peak concentrations and less spreading than those measured at EWs 1 and 3. This behavior suggests differences in hydrodynamic dispersion among these flow zones, as evidenced in the 1-pentanol and preflushing, nonpartitioning

tracer BTCs (discussed above and below, respectively).

During the SPME flood, the physical appearance of the fluids extracted from the test cell followed patterns similar to those evident in the BTCs of Figure 2. Both the resident groundwater and the precursor solution were clear and nearly colorless, but as the microemulsified NAPL started to break through at the extraction wells, a light brown color was evident in the effluent samples. As the concentration of micro-emulsified NAPL increased, the extracted fluids became darker, reaching a dark brown color at maximum concentrations and gradually lightening in color as concentrations decreased. Even the darkest extracted fluids remained isotropically clear, with no sign of macroemulsification; in none of the fluids extracted from the test cell was a separate phase, or mobilized, NAPL observed.

For microemulsification, wherein droplets of NAPL are homogeneously dispersed within the aqueous phase, the relative mole fractions of the NAPL constituents in the microemulsion should be the same as those in the NAPL itself (14, 30, 31). Thus, in the SPME flood, simultaneous elution of all NAPL constituents was expected. Despite the broad range of hydrophobicities exhibited by the Hill NAPL constituents (characterized by the log octanol−water partitioning coefficient, K_{ow}; see Table 1), they were all eluted from the test cell within a narrow time window. This behavior is demonstrated in the cumulative production curves for each analyte, which have been scaled to their respective calculated zeroth moments (Figure 3). While the constituents were all eluted nearly concurrently, a trend in the order of elution was seen. The first normalized moments of the BTCs are inset in Figure 3. Generally, the least hydrophobic contaminants were eluted first, followed by contaminants of increasing hydrophobicity. This behavior is currently being investigated through a detailed analysis of the contaminant BTCs measured at the 96 MLSs.

Rate-Limited Dissolution. Under rate-limited conditions, as the flushing fluid residence time is increased, through either reduced flow rates or flow interruption, solubilization is increased due to greater contact time between the NAPL and the solubilizing agent (12). The SPME precursor residence time was varied by interrupting the flow for periods of 24 h at approximately 4 PV (22.8 kL), 32 h at 6 PV (35.7 kL), and 67 h at 9 PV (54.3 kL). Noticeable changes in target NAPL constituent concentrations were measured at only one of the extraction wells (EW 1) and only following the final interrupt at 54.3 kL (Figure 2). This result suggests that either equilibrium conditions or rate-limited mass transfer processes were too slow to be evidenced over the time scale measured.

Elution of Precursor Solution. After 9 PV, the injection fluid was switched from the SPME precursor solution to a 3% solution of surfactant only. One pore volume of the surfactant solution was injected to facilitate the removal of 1-pentanol from the test cell; this was followed by 6.5 PV of water flooding. After water flooding, the 1-pentanol concentrations at EW 2 had been reduced to 0.5% of C_o, while concentrations were 2% of C_o at EW 1 and 1% of C_o at EW 3. Following the postflushing partitioning tracer test, during which an additional 10 PV of water was flushed through the cell, 1-pentanol concentrations in all three extraction wells were below 1 mg/L.

Soil Cores. Soil concentration profiles of several target NAPL constituents, measured both before and after SPME flushing, are presented in Figure 4. The NAPL smear zone is evident in the preflushing data, wherein the maximum contaminant concentrations are centered around the approximate position of the regional water table (7 m bgs or 1 m above the clay confining unit). A visual comparison of the pre- and postflushing data indicates a dramatic reduction in the target analyte concentrations.
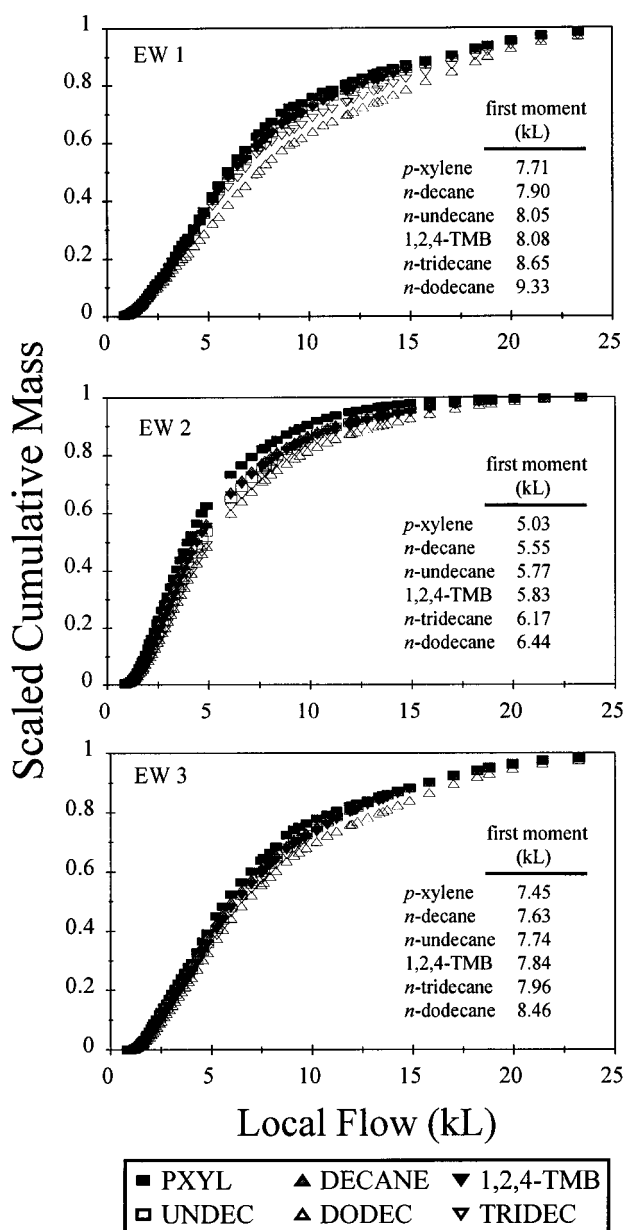

FIGURE 3. Cumulative production curves for the target NAPL constituents, each scaled to its respective calculated zeroth moment. First normalized moments are inset.

Arithmetic average concentrations of the target constituents are presented in Table 2 for soil samples collected within the flushed zone both before and after SPME flushing. Data for those constituents with preflushing average concentrations of less than 0.1 mg/kg are not presented here. Note that the concentrations were significantly higher for *n*-undecane, *n*-decane, and 1,3,5-trimethylbenzene (1,3,5-TMB) than for the other components. The results for these more prevalent constituents are considered to be more reliable than those of the other constituents present only in very small amounts.

Partitioning Tracer Tests. Inspection of the tracer BTCs (Figure 5) reveals substantially less retardation of 2,2-DMP in the postflushing test than in the preflushing test for all three EWs. The swept volumes and the estimated NAPL content within those swept volumes were determined for each extraction well (Table 3). The swept volumes of EW 1 and EW 3 were approximately equal, and both were larger than the EW 2 swept volume. However, the EW 1 swept volume contained the most NAPL, which was evidenced in
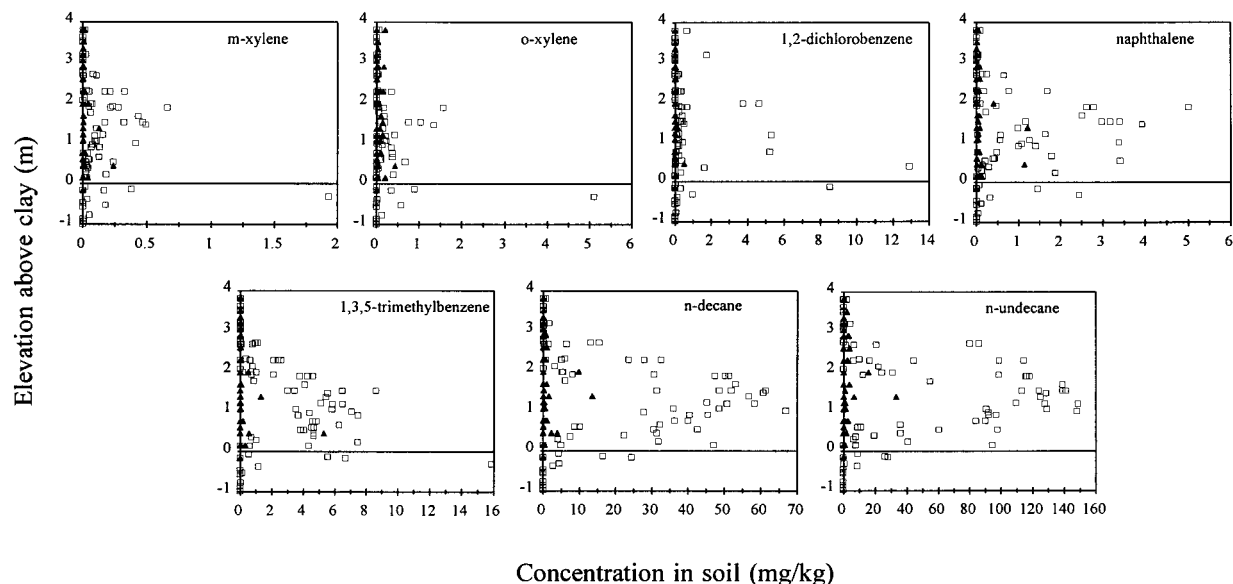
Concentration in soil (mg/kg)

FIGURE 4. Soil concentration profiles before (□) and after (▲) SPME flushing for selected NAPL constituents (determined from methylene chloride extracts of soil core samples).
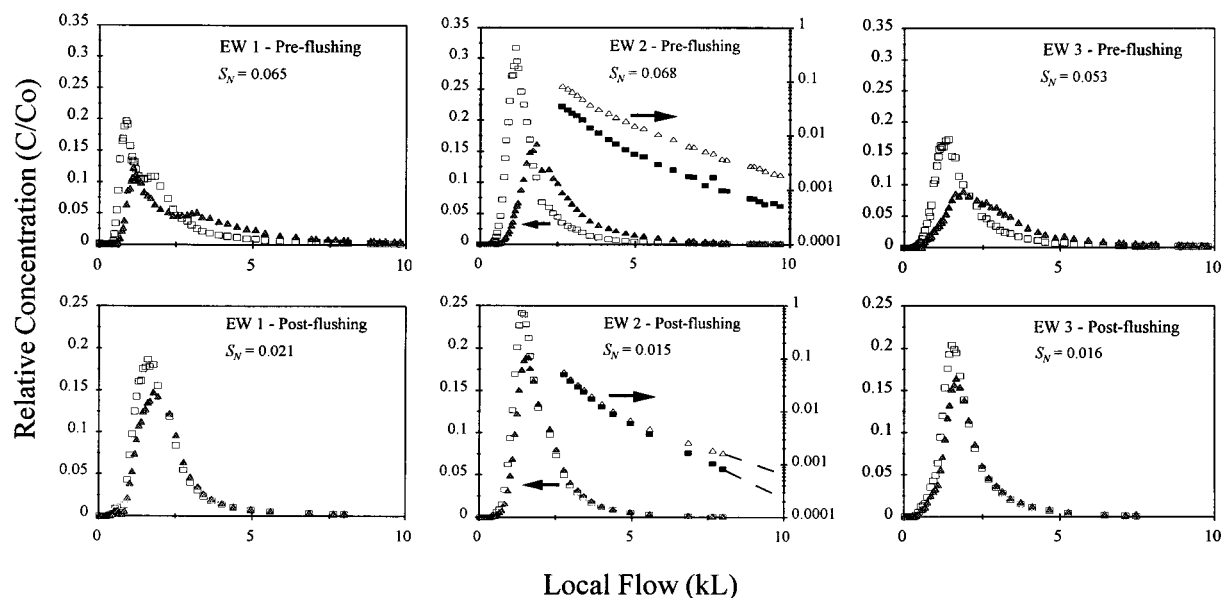

Local Flow (kL)

FIGURE 5. Tracer BTCs at all three EWs for pre- and postflushing tracer tests; methanol (□) was the nonpartitioning tracer and 2,2-dimethyl-3-pentanol (▲) was the partitioning tracer. On the EW 2 graphs, the distal portions of the BTCs are replotted on log-scale on the secondary y-axis; dashed lines are exponential extrapolations.

the greater mass of NAPL constituents removed from EW 1 than from EWs 2 and 3 (Table 1). Also, as seen in the NAPL constituent BTCs, the EW 2 BTCs showed higher peak concentrations and less spreading than those measured at EWs 1 and 3. As discussed above, this was likely due to the sheet-pile corrugations along the flow paths of EWs 1 and 3.

Discussion of NAPL Removal Effectiveness

The evaluation of the effectiveness of the SPME flushing experiment was confounded by the complex composition of the NAPL, leading to inconsistent results from the different removal effectiveness characterization methods.

The NAPL removal effectiveness of the SPME flood was determined from the soil core data by the fraction reduction in average soil concentration of the target NAPL constituents (Table 2). For the NAPL constituents with substantial initial amounts (i.e., preflushing average soil concentrations of >1

mg/kg), NAPL removal effectiveness values were greater than 90%.

The NAPL removal effectiveness was determined from partitioning tracers by the fraction reduction in NAPL saturation. The cell-average reduction in S_N was 72% (Table 3). The NAPL saturations presented in Table 3 were calculated with extrapolated BTCs. Using the unextrapolated data, the cell-average pre- and postflushing NAPL saturations were 0.058 and 0.011, respectively, resulting in a NAPL removal effectiveness of 81%. However, we believe the extrapolated data to be more realistic because extrapolation has been shown to reduce moment estimation errors introduced through BTC tail truncation (13). For illustrative purposes, the distal portions of the EW 2 partitioning and nonpartitioning tracer BTCs in Figure 5 are replotted on a log scale on the secondary y-axis.

NAPL removal effectiveness values were determined from an extraction well mass balance by dividing the amount of

TABLE 3. Pre- and Postflushing NAPL Content in the Swept Volumes of Each Well As Determined from Partitioning Tracer Tests

		EW 1	EW 2	EW 3	total
preflushing[a]	swept volume (kL)	2.21	1.62	2.21	6.04
	NAPL saturation, S_N	0.065	0.068	0.053	0.061[b]
	NAPL volume (kL)	0.153	0.118	0.125	0.396
postflushing	swept volume (kL)	2.17	1.88	2.04	6.09
	NAPL saturation, S_N	0.021	0.015	0.016	0.017[b]
	NAPL volume (kL)	0.047	0.029	0.033	0.109
	fraction reduction of S_N	0.68	0.78	0.70	0.72[b]

[a] Swept volumes were determined from nonpartitioning tracer temporal first moments multiplied by a flow rate of 1.2 L/min at each well. NAPL saturations were determined from partitioning tracer retardation using relationships presented elsewhere (20, 21). NAPL volumes were determined from $V_s S_N/(1 - S_N)$, where V_s is the swept volume. [b] Volume-weighted average of the three extraction wells.

TABLE 4. NAPL Removal Effectiveness, Determined from Extraction Well BTCs and Estimates of the Initial Amount of NAPL from both Partitioning Tracer and Soils Data

	source of initial mass estimate	
NAPL constituent	partitioning tracers	soil cores[a]
p-xylene	0.60	
1,2,4-trimethylbenzene	0.74	
n-decane	0.68	0.61[b]–1.54[c]
n-undecane	0.57	0.68[b]–1.72[c]
n-dodecane	0.56	
n-tridecane	0.70	

[a] Of the constituents listed here, only *n*-decane and *n*-undecane were measured in the soil cores. [b] Obtained using an effective bulk density of 1.7 g/cm³. [c] Effective bulk density of 0.66 g/cm³.

NAPL removed by the initial amount present. The volume of NAPL removed from the test cell was estimated by dividing the mass of each constituent removed through the extraction wells (Table 1) by the mass fractions of the constituents in the NAPL and the NAPL density (0.88 g/cm³). The initial amount of NAPL present as determined from partitioning tracers is shown in Table 3. Soil core data were also used to estimate the initial amount of NAPL present, but of the NAPL constituents that were common to the extraction well and soil core analyses, only *n*-decane and *n*-undecane yielded reliable chromatographic peaks in the effluent samples. The total mass of these two constituents initially present was calculated by multiplying the preflushing cell-average soil concentrations (Table 2) by the total mass of soil in the flushed zone, estimated from the cell area (14.9 m²), an average saturated depth of 3.0 m, and the soil bulk density. The soil concentrations reported in Table 2 are representative of primarily the sand fraction of the aquifer, but the field soil contained a substantial fraction of gravel and cobbles. Therefore, the effective bulk density was estimated to be between 1.7 g/cm³, a standard value for sandy soils (32), and 0.66 g/cm³, equivalent to the standard value scaled by the ratio of the measured porosity (0.14) to the expected porosity for sandy soils (0.36).

The extraction well mass balance determined using partitioning tracers to estimate the initial NAPL volume yielded NAPL removal effectiveness values of 55−75% (Table 4). The mass balance obtained using soil core data to estimate the initial amounts of *n*-decane and *n*-undecane yielded NAPL removal effectiveness estimates of 60−175%. These results demonstrate that determinations of remediation effectiveness made using extraction well BTCs, where the mass removed and the initial mass are determined with different characterization techniques, may exhibit more inconsistency than methods where initial and final contaminant amounts are measured with the same technique, as with the partitioning tracer and soil core methods.

Soil samples collected from the test cell during preflushing coring appeared to be completely coated with the NAPL.

Soils collected during postflushing coring did not appear to be coated with NAPL but appeared to be stained black, especially when compared to uncontaminated aquifer materials collected at the site. This result is consistent with laboratory evidence from column studies using contaminated soil from the field site and the same SPME precursor (19). After 5 PV of SPME flushing, the contaminated soil column was flushed with hexane, and no NAPL constituents were found in the hexane effluent, indicating that all compounds soluble in organic solvents had been removed from the soil. However, pre- and postflushing partitioning tracer tests indicated that only 70% of the NAPL had been removed. Inspection of the flushed soil revealed a dark coating. This residue was not solubilized by either the SPME precursor or hexane but did serve as a sorbent for the partitioning tracers (no retardation of tracers was found on uncontaminated field soil).

Thus, while soil core data indicate that >90% of the mass of the target NAPL constituents was removed by the SPME flood, partitioning tracer and observational data indicate that an anthropogenic residue was left behind. It remains to be determined whether better agreement would be found between different techniques for assessing the effectiveness of SPME flushing at sites with less complex NAPLs.

Supporting Information Available

An appendix containing text and 3 figures plus captions (9 pp) will appear following these pages in the microfilm edition of this volume of the journal. Photocopies of the Supporting Information from this paper or microfiche (105 × 148 mm, 24× reduction, negatives) may be obtained from Microforms Office, American Chemical Society, 1155 16th St. NW,

Literature Cited

(1) Rao, P. S. C.; Annable, M. D.; Sillan, R. K.; Dai, D.; Hatfield, K.; Graham, W. D.; Wood, A. L.; Enfield, C. G. *Water Resour. Res.* **1997**, *33* (12), 2673−2686.

(2) Brown, C. L.; Delshad, M.; Dwarakanath, V.; Jackson, R. E.; Londergan, T.; Meinardus, H. W.; McKinney, D. C.; Oolman, T.; Pope, G. A.; Wade, W. H. *Environ. Sci. Technol.* Submitted for publication.

(3) Fountain, J. C.; Starr, R. C.; Middleton, T.; Beikirch, M.; Taylor, C.; Hodge, D. *Ground Water* **1996**, *34* (5), 910−916.

(4) Falta, R. W.; Brame, S. E.; Lee, C. M.; Coates, J. T.; Wright, C.; Price, S.; Haskell, P.; Roeder, E. A field test of NAPL removal by high molecular weight alcohol injection. *Proceedings of the Non-Aqueous Phase Liquids (NAPLs) in Subsurface Environment: Assessment and Remediation*; Reddi, L. N., Ed.; ASCE: Washington, DC, November 12−14, 1996; pp 257−268.

(5) Shah, D. O., Ed. *Surface Phenomena in Enhanced Oil Recovery*; Plenum Press: New York, 1981.

(6) Lake, L. W. *Enhanced Oil Recovery*; Prentice Hall: Englewood Cliffs, NJ, 1989.

(7) Peters, C. A.; Luthy, R. G. *Environ. Sci. Technol.* **1993**, *27* (13), 2831−2843.

(8) Brandes, D.; Farley, K. J. *Water Environ. Res.* **1993**, *65* (7), 869−878.

(9) Augustijn, D. C. M.; Jessup, R. E.; Rao, P. S. C.; Wood, A. L. *J. Environ. Eng.* **1994,** *120* (1), 42−57.

(10) Imhoff, P. T.; Gleyzer, S. N.; McBride, J. F.; Vancho, L. A.; Okuda, I.; Miller, C. T. *Environ. Sci. Technol.* **1995**, *29* (8), 1966−1976.

(11) Abdul, A. S.; Gibson, T. L.; Ang, C. C.; Smith, J. C.; Sobczynski, R. E. *Ground Water* **1992**, *30* (2), 219−231.

(12) Pennell, K. D.; Abriola, L. M.; Weber, W. J., Jr. *Environ. Sci. Technol.* **1993**, *27*, 2332−2340.

(13) Jin, M. Ph.D. Dissertation, University of Texas at Austin, Austin, TX, 1995.

(14) Shiau, B.-J.; Sabatini, D. A.; Harwell, J. H.; Vu, D. Q. *Environ. Sci. Technol.* **1996**, *30* (1), 97−103.

(15) Pennell, K. D.; Pope, G. A.; Abriola, L. M. *Environ. Sci. Technol.* **1996**, *30* (4), 1328−1335.

(16) Sabatini, D. A.; Knox, R. C.; Harwell, J. H. *Surfactant-Enhanced DNAPL Remediation: Surfactant Selection, Hydraulic Efficiency, and Economic Factors*; Environmental Research Brief, EPA/600/S-96/002; National Risk Management Research Laboratory, U.S. EPA: Ada, OK, 1996.

(17) Augustijn, D. C. M.; Rao, P. S. C. In *Emerging Technologies in Hazardous Waste Management V*; Tedder, D. W., Pohland, F. G., Eds.; American Chemical Society: Washington, DC, 1995.

(18) Ouyang, Y.; Mansell, R. S.; Rhue, R. D. *J. Hazard. Mater.* **1996**, *46*, 23−35.

(19) Rhue, R. D.; Annable, M. D.; Rao, P. S. C. *Lab and Field Evaluation of Single-Phase Microemulsions (SPME) for Enhanced In Situ Remediation of Contaminated Aquifers. Phase I: Laboratory Studies for Selection of SPME Precursors*; AATDF Report; University of Florida: Gainesville, FL, 1997.

(20) Jin, M.; Delshad, M.; Dwarakanath, V.; McKinney, D. C.; Pope, G. A.; Sepehrnoori, K.; Tilburg, C. E.; Jackson, R. E. *Water Resour. Res.* **1995**, *31* (5), 1201−1211.

(21) Annable, M. D.; Rao, P. S. C.; Graham, W. D.; Hatfield, K.; Wood, A. L. *J. Environ. Eng.* In press.

(22) Rosen, M. J. *Surfactants and Interfacial Phenomena*, 2nd ed.; John Wiley & Sons: New York, 1989.

(23) Baran, J. R., Jr.; Pope, G. A.; Wade, W. H.; Weerasooriya, V. *Environ. Sci. Technol.* **1994**, *28* (7), 1361−1366.

(24) Pithapurwala, Y. K.; Sharma, A. K.; Shah, D. O. *J. Am. Oil Chem. Soc.* **1986**, *63* (6), 804−813.

(25) Martel, R.; Gélinas, P. J.; Desnoyers, J. E.; Masson, A. *Ground Water* **1993**, *31* (5), 789−800.

(26) Martel, R.; Gélinas, P. J. *Ground Water* **1996**, *34* (1), 143−154.

(27) Huh, C. *J. Colloid Interface Sci.* **1979**, *71*, 408.

(28) Montgomery Watson Inc. *Hill Air Force Base, Utah, Phase I Work Plan for Eight Treatability Studies at Operable Unit 1*; Montgomery Watson: Salt Lake City, UT, 1995.

(29) Valocchi, A. J. *Water Resour. Res.* **1985**, *21* (6), 808−820.

(30) Salager, J. L.; Bourrel, M.; Schechter, R. S.; Wade, W. H. *Soc. Pet. Eng. J.* **1979**, *19* (5), 271−278.

(31) Puerto, M. C.; Reed, R. L. *Soc. Pet. Eng. J.* **1983**, *23*, 669−682.

(32) Freeze, R. A.; Cherry, J. A. *Groundwater*; Prentice Hall: Englewood Cliffs, NJ, 1979.

(33) Sangster, J. *J. Phys. Chem. Ref. Data* **1989**, *18* (3), 1111−1229.